Antibody-Maytansinoid Conjugates Are Activated in Targeted Cancer Cells by Lysosomal Degradation and Linker-Dependent Intracellular Processing

Hans K. Erickson, Peter U. Park, Wayne C. Widdison, Yelena V. Kovtun, Lisa M. Garrett, Karen Hoffman, Robert J. Lutz, Victor S. Goldmacher, and Walter A. Blättler

ImmunoGen, Inc., Cambridge, Massachusetts

Abstract

Antibody-drug conjugates are targeted anticancer agents consisting of a cytotoxic drug covalently linked to a monoclonal antibody for tumor antigen–specific activity. Once bound to the target cell-surface antigen, the conjugate must be processed to release an active form of the drug, which can reach its intracellular target. Here, we used both biological and biochemical methods to better define this process for antibody-maytansinoid conjugates. In particular, we examined the metabolic fate in cells of huC242-maytansinoid conjugates containing either a disulfide linker (huC242-SPDB-DM4) or a thioether linker (huC242-SMCC-DM1). Using cell cycle analysis combined with lysosomal inhibitors, we showed that lysosomal processing is required for the activity of antibody-maytansinoid conjugates, irrespective of the linker. We also identified and characterized the released maytansinoid molecules from these conjugates, and measured their rate of release compared with the kinetics of cell cycle arrest. Both conjugates are efficiently degraded in lysosomes to yield metabolites consisting of the intact maytansinoid drug and linker attached to lysine. The lysine adduct is the sole metabolite from the thioether-linked conjugate. However, the lysine metabolite generated from the disulfide-linked conjugate is reduced and *S*-methylated to yield the lipophilic and potently cytotoxic metabolite, *S*-methyl-DM4. These findings provide insight into the mechanism of action of antibody-maytansinoid conjugates in general, and more specifically, identify a biochemical mechanism that may account for the significantly enhanced antitumor efficacy observed with disulfide-linked conjugates. (Cancer Res 2006; 66(8): 4426-33)

Introduction

Antibody-drug conjugates are designed to selectively eliminate cancer cells that express the target cell surface antigen (for recent reviews, see refs. 1–3). Several conjugates are currently in clinical evaluation (3) and one conjugate, gemtuzumab ozogamicin, is licensed for the treatment of refractory acute myeloid leukemia (4).

Antibody-drug conjugates are structurally composed of a monoclonal antibody that binds specifically to a target antigen, a small chemical cytotoxic drug, and a linker that stably connects the two. We have developed conjugates that contain maytansinoid drugs, which are derivatives of the natural cytotoxic polyketide, maytansine (5). In particular, we have developed maytansinoid conjugates of the humanized monoclonal antibody, huC242, which binds to the CanAg antigen expressed on colorectal, pancreatic, and certain non–small cell lung cancers (6). During the preclinical development, we compared several conjugates of huC242 that differed in the chemical nature of the linker between huC242 and the maytansinoid and established that one conjugate, huC242-SPDB-DM4, had the highest activity in several human xenograft tumor models in mice and the widest therapeutic window as defined by the largest difference between the minimal effective dose and the maximal tolerated dose. Based on these results, huC242-SPDB-DM4 was selected for clinical development and is currently being tested in a phase I trial.

Here, we report that the huC242-maytansinoid conjugate, huC242-SMCC-DM1, with a "noncleavable" linker containing a thioether bond was at least as potent *in vitro* as the selected conjugate, huC242-SPDB-DM4, which has a "cleavable" linker containing a disulfide bond. This was surprising because huC242-SMCC-DM1 displayed significantly lower *in vivo* activity in multiple xenograft tumor models. To investigate this conundrum, we undertook a series of experiments to elucidate the mechanism of cell killing by the conjugates. The results delineate an activation process, for both conjugates, that requires lysosomal degradation of the antibody component of the conjugate. However, distinct maytansinoid metabolites produced by intracellular processing of huC242-SPDB-DM4 were identified and characterized, providing a likely mechanism for its superior antitumor efficacy.

Materials and Methods

Materials. RPMI 1640 and glutamine were from Cambrex Bioscience (Walkersville, MD). Ultima Flo M scintillation fluid was from Perkin-Elmer Life and Analytical Sciences (Wellesley, MA) Gentamicin sulfate was from Life Technologies (Gaithersburg, MD). *N*-Ethylmaleimide and all other chemicals were obtained from Sigma (St. Louis, MO). All antibodies used, huC242, Tras, and huB4, are humanized IgG1 antibodies. The maytansinoids [^{3}H]DM4, D-[^{3}H]DM4, *S*-methyl-DM4, lysine-N^{ϵ}-SMCC-DM1, and lysine-N^{ϵ}-SPDB-DM4, and the conjugates, huC242-SPDB-[^{3}H]DM4, huC242-SMCC-[^{3}H]DM4, Tras-SMCC-[^{3}H]DM4, and huB4-SPDB-[^{3}H]DM4, were prepared at ImmunoGen following published procedures (7, 8).

Treatment of COLO 205 cells with antibody-drug conjugates. COLO 205 cells (6×10^6) suspended in 3 mL culture medium containing an antibody-drug conjugate at a concentration of 10^{-7} mol/L of conjugated antibody were incubated at 37°C for 3 to 30 hours. The cells and the medium were then separated by centrifugation (2,000 × *g*, 5 minutes). The supernatant (3 mL) was chilled on ice, mixed with 4 mL ice-cold acetone, and kept at −80°C for at least 1 hour or until further processing. The cells

Note: Supplementary data for this article are available at Cancer Research Online (http://cancerres.aacrjournals.org/).

H.K. Erickson and P.U. Park contributed equally to this work.

Requests for reprints: Hans K. Erickson, ImmunoGen, Inc., 128 Sidney Street, Cambridge, MA 02139. Phone: 617-995-2500; Fax: 617-995-2510; E-mail: hans.erickson@immunogen.com.

doi:10.1158/0008-5472.CAN-05-4489

were suspended in 3 mL HBBS buffer and sedimented by centrifugation, then resuspended in 0.3 mL TBS containing 0.5% bovine serum albumin. At this point, if alkylation was desired for capping of free thiols, *N*-ethylmaleimide was added to 7.5 mmol/L, and the solution was mixed and kept at room temperature for 30 minutes. The cell suspension was then mixed with 0.6 mL ice-cold acetone. The samples were placed at −80°C for at least 1 hour or until further processing. Precipitated protein was removed by centrifugation at 2,500 × *g* and the supernatants were acidified with 5% acetic acid and evaporated to dryness. The samples were dissolved in 0.12 mL of 20% aqueous CH_3CN containing 0.025% trifluoroacetic acid (TFA), aliquots of 0.1 mL were submitted to high-performance liquid chromatography (HPLC).

***In vivo* studies.** The antitumor activity of the conjugates was assessed in female CB-17 severe combined immunodeficient mice (SCID mice; Taconic Labs, Germantown, NY) bearing HT-29 tumors as described previously (9). Conjugates were administered i.v. to groups of six mice.

Cell cycle studies. Exponentially growing COLO 205 cells were resuspended at 1 × 10^5/mL to 2 × 10^5/mL before drug or conjugate treatment. The nuclei of the cells were stained with propidium iodide as previously described (10). DNA content analysis was done using FACSCalibur (Becton Dickinson, San Jose, CA). For each sample, 10,000 events were collected and FL2-A histograms were generated. The cell cycle analysis software, ModFit LT 3.1 (Verity Software House, Topsham, ME) was used to determine the percentage of cells in different phases of the cell cycle.

Analytic methods. All maytansinoids were separated on an analytic C-18 column (0.46 × 25 cm) equilibrated with 20% aqueous CH_3CN containing 0.025% TFA and developed with a linear gradient of 2% CH_3CN/min and a flow rate of 1 mL/min. The effluent was directed to a diode array detector followed either by a Radiomatic 150 β-counter (Perkin-Elmer Life and Analytic Sciences) where the effluent was mixed continuously with 3 mL scintillation cocktail before it was directed to a 0.5 mL flow cell or a Bruker Daltonics Esquire 3000 electrospray mass spectrometer depending on the application. The data sampling interval was 6 seconds. The peak areas of the chromatograms were converted to picomoles as follows: A standard curve to relate the peak of radioactivity (mV^2) on the chromatograms to cpm of tritium was prepared by injecting 1,000 to 50,000 cpm of a stock solution of [^{3}H]DM4 (250 mCi/mmol) diluted in 20% aqueous CH_3CN containing 0.025% TFA. Duplicates for each sample were submitted to HPLC as described above.

Results

***In vitro* potency and *in vivo* activity of huC242-maytansinoid conjugates.** The disulfide-linked antibody-maytansinoid conjugate, huC242-SPDB-DM4, and the thioether-linked conjugate, huC242-SMCC-DM1, were first assayed for their cytotoxic potency against antigen-positive COLO 205 cells and antigen-negative Namalwa cells (both sensitive to maytansine with IC_{50} values of ~30 to 60 pmol/L for both cell lines) using an 3-(4,5-dimethylthiazol-2-yl)-2,5-diphenyltetrazolium bromide (MTT)–based assay. The conjugates displayed similar potencies with IC_{50} values of 40 pmol/L against COLO 205 cells and 20 to 80 nmol/L against Namalwa cells upon a 4-day exposure of the cells to the conjugates (Fig. 1*A*). The antitumor activity of the two conjugates was assessed in SCID mice bearing s.c. HT-29 or COLO 205 tumors (both CanAg-positive human colon adenocarcinoma). The activity of huC242-SPDB-DM4 at a single dose of 50 μg/kg (concentration based on conjugated DM4) in eradicating HT-29 tumors was greater than that of huC242-SMCC-DM1 when administered as five daily injections at a dose of 150 μg/kg/d (Fig. 1*B*). HuC242-SPDB-DM4 also displayed greater activity than huC242-SMCC-DM1 when both were administered as five daily injections at a dose of 150 μg/kg/d in SCID mice bearing COLO 205 tumors (five of five tumor free mice at 122 days compared with two of five tumor free mice at 122 days; data not shown). These results show that although both conjugates display similar cytotoxicity *in vitro*, their efficacy against tumors *in vivo* differs significantly.

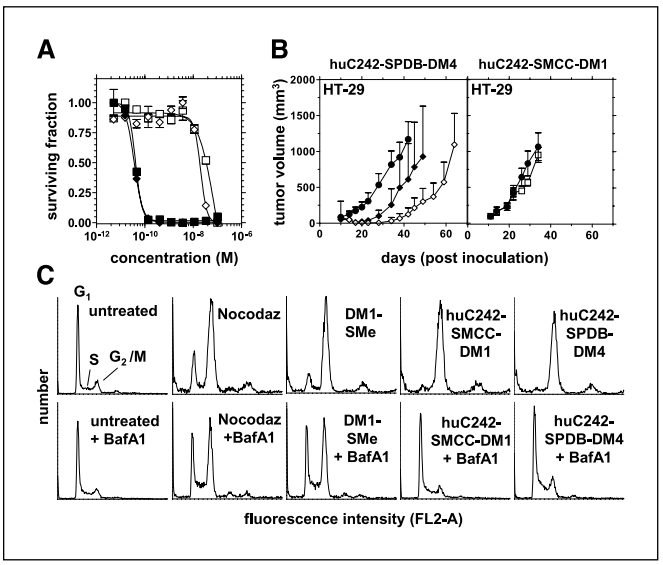

Figure 1. Cytotoxicity of huC242-SPDB-DM4 and huC242-SMCC-DM1 and their effects on the cell cycle progression in the presence of the lysosomal inhibitor BafA1. *A,* surviving fractions of antigen-positive COLO 205 (*closed symbols*) and antigen-negative Nalmawa cells (*open symbols*) were measured using an MTT assay after exposure to different concentrations of huC242-SPDB-DM4 (*diamonds*) or huC242-SMCC-DM1 (*squares*) for 4 days, and plotted versus conjugate concentrations. *B,* antitumor activities of huC242-SPDB-DM4 and huC242-SMCC-DM1 in SCID mice bearing HT-29 human colon tumor xenografts. Doses are based on the amount of conjugated DM4 or DM1. Tumor-bearing mice were treated with PBS (*closed circles, left* and *right*), a single dose of 50 μg/kg huC242-SPDB-DM4 (*open diamonds*), 150 μg/kg huC242-SPDB-DM4 (*closed diamonds*), or five daily injections of huC242-SMCC-DM1 at a dose of 150 μg/kg (*open squares*). *C,* FACS histograms (FL2-A) display DNA contents of asynchronous, exponentially growing COLO 205 cells treated for 20 hours with 0.66 μmol/L nocodazole, 10^{-8} mol/L DM1-SMe, 3 × 10^{-9} mol/L huC242-SMCC-DM1, or 3 × 10^{-9} mol/L huC242-SPDB-DM4 in the presence of 30 nmol/L BafA1 or no treatment.

Effect of lysosomal inhibitors on cell cycle arrest induced by huC242-maytansinoid conjugates. Maytansinoids inhibit tubulin polymerization, which leads to cell cycle arrest in the G_2-M phase (11); therefore, we checked if this activity was also present in both conjugates. Samples of asynchronously growing cells were exposed to conjugate (3 nmol/L), DM1-SMe (10 nmol/L; see Fig. 5 for structure), or nocodazole (0.66 μmol/L), another inhibitor of microtubule polymerization, at 37°C for 20 hours. The DNA content of the cells was then analyzed by flow cytometry. In cultures treated with nocodazole or DM1-SMe, >50% of the cells were arrested in the G_2-M phase (Fig. 1*C*, *first row*), compared with only 10% of untreated COLO 205 cells (typically ~60% in G_1 and 30% in S). In samples treated with either of the two conjugates, ~70% to 80% of the cells were arrested at the G_2-M phase, indicating that the cell cycle effects of maytansinoid conjugates are similar to those of the free maytansinoids (Fig. 1*C*). No cell cycle arrest was induced by the conjugates in cells lacking the target antigen (data not shown).

To test whether uptake and processing of conjugates through lysosomes was necessary for their activity against cancer cells, we examined G_2-M arrest induced by conjugates in the presence of bafilomycin A1 (BafA1), a lysosomal inhibitor. BafA1 selectively

inhibits V-ATPase, a proton pump present in endosomes and lysosomes, which leads to neutralization of the pH in these vesicles (12, 13). The pH neutralization blocks trafficking from late endosomes to lysosomes and lysosomal processing, yet modestly affects the rate of internalization and recycling and does not inhibit trafficking between endosomes and trans-Golgi (14–16). We also found that the rate of internalization of a fluorescently modified huC242 was not affected by BafA1 (data not shown). The treatment of COLO 205 cells with BafA1 alone did not significantly alter the distribution of cells between the phases of the cell cycle (Fig. 1*C*). However, in the presence of BafA1, G_2-M arrest induced by either huC242-SMCC-DM1 or huC242-SPDB-DM4 was almost completely abolished (6-9% in G_2-M; Fig. 1*C*). In contrast, BafA1 treatment had a modest effect on the extent of G_2-M arrest caused by the free maytansinoid, DM1-SMe or by nocodazole (37-39% in G_2-M; Fig. 1*C*). Similar results were also found when chloroquine, another lysosomal inhibitor that neutralizes pH by a different mechanism (16, 17), was used (Supplementary Fig. S1). These findings were the first indication of the importance of lysosomal processing in the activation of both huC242-SMCC-DM1 and huC242-SPDB-DM4.

Isolation of maytansinoid metabolites from huC242-maytansinoid conjugates. To examine the fate of the maytansinoid drug upon incubation of target cells with an antibody-maytansinoid conjugate, we prepared conjugates with maytansinoids that were ^{3}H-labeled at the C-20 methoxy group (see Fig. 5). Radiolabeled maytansinoid conjugates, huC242-SPDB-[^{3}H]DM4 (250 mCi/mmol) and huC242-SMCC-[^{3}H]DM1 (214 mCi/mmol), exhibit *in vitro* cytotoxicities similar to nonradiolabeled conjugate samples (data not shown). Cultures of 2×10^6 COLO 205 cells were exposed to 10^{-7} mol/L ^{3}H-labeled conjugates for periods of 5, 9, and 26 hours, separated into cell and conditioned medium fractions, and each sample was extracted with acetone. We determined that cells treated under these conditions remained viable with intact plasma membranes for at least the first 26 hours of exposure as determined by trypan blue staining (data not shown). The acetone extracts were analyzed for ^{3}H-labeled metabolites by reversed-phase HPLC. The chromatograms in Fig. 2*A* display signals for the amount of radioactivity in the acetone-extracted samples from the thioether-linked huC242-SMCC-[^{3}H]DM1-treated cells. A control was prepared from an acetone extract of the conjugate used in the experiment to identify free maytansinoid species present in the huC242-SMCC-[^{3}H]DM1 sample before the exposure to cells (Fig. 2*A, g*). Two new, partially separated peaks of radioactivity with retention times of ~18.7 and 19.2 minutes, respectively, were identified in extracts from cell pellets. These metabolites are readily detectable after a 5-hour exposure, and increase by 9 and 26 hours (Fig. 2*A, a, c, e*). These same metabolites were also detectable in the culture medium but not until the 9-hour time point, and then were readily detectable in the 26-hour sample. In separate experiments, the two metabolites were isolated and found by mass spectrometry (MS) to be the two isomers of lysine-N^{ϵ}-SMCC-[^{3}H]DM1 (*R* or *S* configuration at the carbon of the thioether bond formed in the conjugation reaction; both peaks M+ = 1,103.5; M + Na = 1,125.5).

The results from an analogous experiment with the disulfide-linked huC242-SPDB-[^{3}H]DM4 conjugate are shown in Fig. 2*B*. Three distinct peaks of radioactivity with retention times of 20.5, 26.5, and 27 minutes were observed in the chromatograms derived from the cell pellets treated with huC242-SPDB-[^{3}H]DM4 for 5 and 9 hours (Fig. 2*B, a* and *c*). Cells treated for 26 hours yielded largely one peak with a retention time of 27 minutes (Fig. 2*B, e*), indicating that the metabolites eluting at 20.5 and 26.5 minutes had either been converted to the metabolite eluting at 27 minutes or were no longer present in the cells. The peak at 26.5 minutes has the same retention time as DM4. To further study this metabolite and to assess whether any of the other metabolites contained a free sulfhydryl group, an acetone extract from a 9-hour exposure was treated with

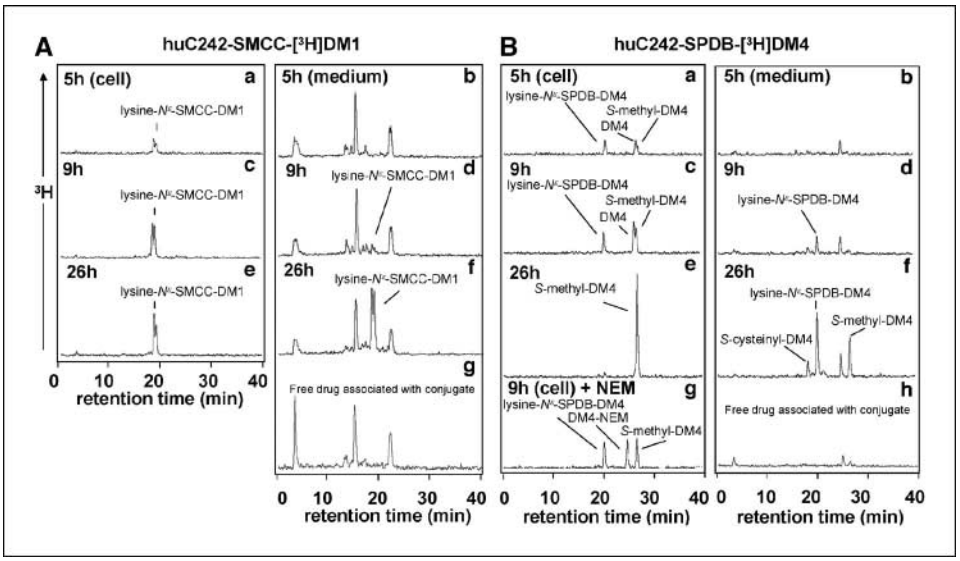

Figure 2. Maytansinoid metabolites formed upon treatment of COLO 205 cells with huC242-SMCC-[^{3}H]DM1 (*A*) or huC242-SPDB-[^{3}H]DM4 (*B*). Metabolites were extracted with acetone from the cell pellet and the spent medium, respectively, and then analyzed by HPLC. The effluent from the column was monitored for tritium using an in-line flow scintillation analyzer with an output in mV^2; thus, the chromatograms show retention time on the abscissa and mV^2 as a measure of [^{3}H] on the ordinate. *a* to *f*, chromatograms associated with the medium and cell pellets from COLO 205 cells that were treated for 5, 9, and 26 hours with huC242-SMCC-[^{3}H]DM1 (*A*) or huC242-SPDB-[^{3}H]DM4 (*B*). *g* (*A*) and *h* (*B*), chromatograms obtained from the acetone extract of the huC242-SMCC-[^{3}H]DM1 and huC242-SPDB-[^{3}H]DM4 conjugate sample, respectively, used in the experiment. *g* (*B*), chromatogram derived from cells that were treated equally to the cell pellet from the 9-hour incubation (as in *c*), except that the sample was additionally exposed to *N*-ethylmaleimide (*NEM*) before chromatography to alkylate any sulfhydryl groups.

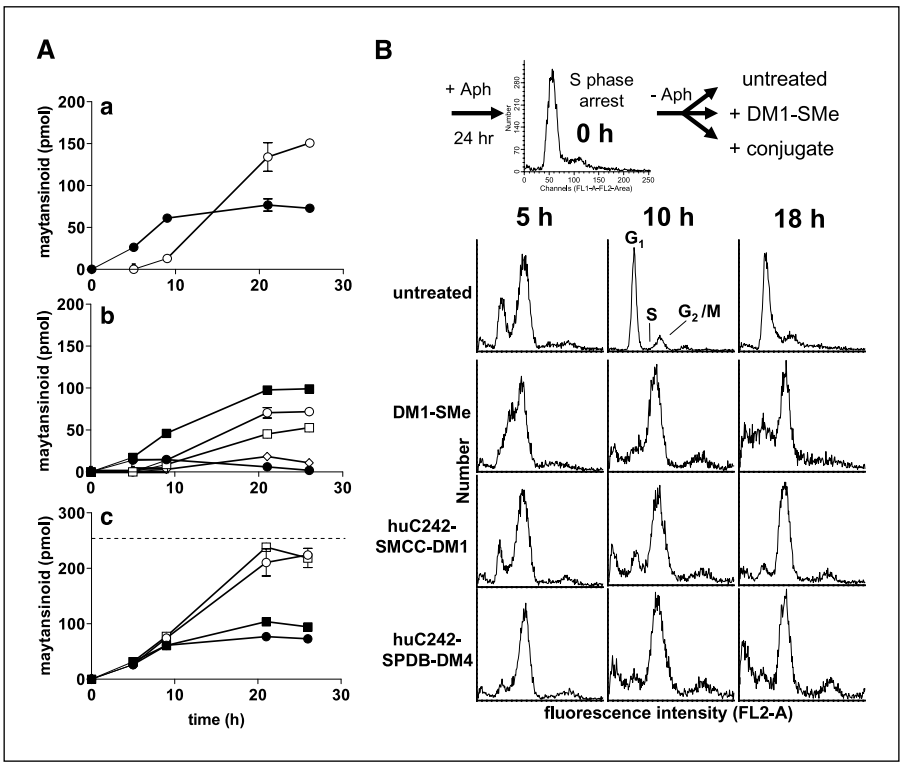

Figure 3. Accumulation of maytansinoid metabolites inside and outside of COLO 205 cells treated with ^{3}H-maytansinoid conjugates and their correlation with mitotic arrest. *A,* areas associated with the peaks of radioactivity for the metabolites in Fig. 2 were quantified and converted to picomoles as described in Materials and Methods. *a* to *c,* changes in the amount of various metabolites in the samples over a 26-hour incubation period. *a,* accumulation of lysine-N^{ϵ}-SMCC-DM1 in the medium (*open circles*) and cells (*closed circles*) following treatment of COLO 205 cells with huC242-SMCC-[^{3}H]DM1. *b,* changes in the amounts of maytansinoid metabolites in the cell pellet (*closed symbols*) and in the medium (*open symbols*) following treatment of COLO 205 with huC242-SPDB-[^{3}H]DM4: *S*-methyl-DM4 + DM4 (*squares*), lysine-N^{ϵ}-SPDB-DM4 (*circles*), *S*-cysteinyl-DM4 (*diamonds*). *c,* change of the sum of all metabolites present for both conjugates, huC242-SMCC-[^{3}H]DM1 (*circles*) and huC242-SPDB-[^{3}H]DM4 (*squares*), either in the cell pellet (*solid symbols*) or in the cell pellet and medium together (*open symbols*). *B,* COLO 205 cells were synchronized in S phase with a 24 hours of treatment of 2 μg/mL aphidicolin. The cells were released from S phase by the removal of aphidicolin and incubated with 10^{-8} mol/L DM1-SMe, 3×10^{-9} mol/L huC242-SMCC-DM1, 3×10^{-9} mol/L huC242-SPDB-DM4, or left untreated. FACS analysis was done at 5, 10, and 18 hours after aphidicolin release.

N-ethylmaleimide and then subjected to HPLC (Fig. 2*B, g*). Following alkylation, the peak at 26.5 minutes, observed in the 5- and 9-hour samples, was replaced with a new peak at 25 minutes. This new peak coelutes with a standard of the purified DM4-*N*-ethylmaleimide reaction product (data not shown), suggesting that the metabolite at 26.5 minutes is indeed DM4.

The corresponding chromatograms associated with the conditioned medium from treated cells are displayed in Fig. 2*B* (*b, d*, and *f*). After 5 hours of exposure, no metabolites can be detected; the peaks present are also visible in the control chromatogram of the acetone extract of the conjugate sample (Fig. 2*B, h*). After 9 hours of exposure, however, the unknown metabolite with a retention time of 20.5 minutes that was observed in cells after 5 hours can be detected in the medium, and after 26 hours, two additional metabolites with retention times of 18.5 and 27 minutes were present. The unique metabolite in the medium that elutes at 18.5 minutes was found to have the same retention time as the mixed disulfide between DM4 and cysteine (*S*-cysteinyl-DM4; data not shown). RPMI 1640 contains 0.21 mmol/L cystine, and separate experiments have shown that DM4 under these conditions reacts rapidly ($t_{1/2}$ < 1 hour) to form *S*-cysteinyl-DM4 through a thiol-disulfide interchange reaction (data not shown). Thus, the *S*-cysteinyl-DM4 disulfide compound would be expected to form in the medium if the DM4 observed in the cell pellet leaves the cells. To further test whether any of the metabolites in the medium were disulfide compounds, a cell supernatant sample from a 26-hour exposure was divided into two equal portions of which one was subjected directly to chromatography, and the other portion was treated with DTT and selenol before chromatography to reduce all disulfide bonds (18). Following reduction, all of the peaks of radioactivity in the chromatograms disappeared except the peak eluting at 27 minutes and a single new peak appeared with a retention time of 26.5 minutes, which is that of DM4 (Supplementary Fig. S2). Thus, the metabolites eluting at 18.5 and 20.5 minutes, but not the metabolite at 27 minutes, are DM4 species containing a disulfide-linked substituent. In separate experiments, the unknown metabolites eluting at 20.5 and 27 minutes were found to have a mass consistent with lysine-N^{ϵ}-SPDB-DM4 (M + Na = 1048.4) and *S*-methyl-DM4 (M + Na = 816.4/M + K = 832.5), respectively.

In the above experiments, 2×10^6 COLO 205 cells were incubated in 3 mL medium containing 10^{-7} mol/L conjugate. From this large amount of conjugate, <20% of the conjugate-bound maytansinoid was recovered in the identified maytansinoid metabolites after incubation with the cells for 26 hours (Fig. 3*A*, *c*; dotted line represents 20% level). In a separate experiment following the fate of huC242-SPDB-[^{3}H]DM4 that was bound to cells at 4°C, we determined that within a 22-hour period at 37°C, 73% of the conjugated DM4 bound to COLO 205 cells was converted into the four maytansinoid metabolites—DM4, *S*-cysteinyl-DM4, lysine-N^{ϵ}-SPDB-DM4, and *S*-methyl-DM4 (Supplementary Fig. S3). We conclude that these metabolites represent the majority (if not all) of the metabolites formed in the cellular activation process. Moreover, production of these maytansinoid metabolites was not observed when COLO 205 cells were incubated with disulfide-linked or SMCC-linked maytansinoid conjugates, which do not bind target antigens on these cells (Supplementary Fig. S4).

The kinetics for the accumulation of metabolites and cell cycle arrest. The peak areas of radioactivity associated with the metabolites generated from huC242-SMCC-[^{3}H]DM1 and from huC242-SPDB-[^{3}H]DM4 (Fig. 2) were determined and converted to picomoles of maytansinoid as described in Materials and Methods. The results are shown in Fig. 3*A* as accumulation of the maytansinoid metabolites over time from the addition of the conjugates to the cells (T = 0). Figure 3*A* (*a*) shows the

accumulation of lysine-N^{ϵ}-SMCC-DM1, the single metabolite from huC242-SMCC-[^{3}H]DM1, in the cell pellet and in the medium. The concentration of the metabolite in the cells reaches a steady state after 9 hours of incubation, which may be due to the saturation of an intracellular binding site. This maytansinoid metabolite begins to appear in the medium at 9 hours, suggesting efficient efflux of the charged lysine-N^{ϵ}-SMCC-DM1 species across the plasma membrane. Figure 3*A* (*b*) shows the accumulation of the three stable metabolites generated from huC242-SPDB-[^{3}H]DM4, in the cell pellet and in the medium. The intracellular amount of the disulfide compound, lysine-N^{ϵ}-SPDB-DM4, declines over the observed period of 26 hours, presumably through disulfide cleavage to DM4 in the intracellular reducing environment, followed by subsequent conversion of the resulting free thiol, DM4, to the stable *S*-methyl-DM4 derivative. Very little, if any, DM4 was observed inside the cells after 9 hours of incubation, indicating rapid methylation probably catalyzed by a methyl transferase. The total intracellular accumulation of metabolites reaches a steady state after 9 hours of exposure to either conjugate and the levels of metabolites at the steady state are about the same for both conjugates (Fig. 3*A*, *c*), suggesting that the conjugates share the same rate-limiting step with respect to production of the metabolites and that these metabolites likely bind to the same intracellular target.

Because only ~9 hours is required for intracellular accumulation of metabolites to reach the steady-state level, we investigated whether G_2-M arrest induced by either conjugate can occur within that time frame. COLO 205 cells were first synchronized with a 24-hour treatment of aphidicolin, a reversible DNA replication inhibitor that blocks cells in S phase (19). Because the majority of the asynchronous population of COLO 205 cells were in G_1 phase, most of the aphidicolin-treated cells arrested in the beginning of S phase, which cannot be distinguished from G_1 phase in the fluorescence-activated cell sorting (FACS) analysis (Fig. 3*B*, *top picture*). The synchronized cells were then released from the arrest by the removal of aphidicolin, and either left untreated, or treated with DM1-SMe or with either conjugate. Untreated cells immediately continue with DNA synthesis, and the majority is in G_2-M phase (59%) after 5 hours (Fig. 3*B*), and has undergone mitosis at 10 hours and are in G_1 phase (76%). In contrast, the majority of cells treated with DM1-SMe or either conjugate are in G_2-M phase (75% to 85%) after 10 and 18 hours, indicating that sufficient amounts of active drug species have accumulated intracellularly to induce mitotic arrest when the aphidicolin-released cells reached mitosis. Therefore, COLO 205 cells require as little as 5 hours, but not more than 10 hours to produce enough of active drug metabolites to cause cell cycle arrest. Thus, the kinetics of G_2-M phase arrest induced by these conjugates correlate with the time required to reach the steady-state level of intracellular accumulation of the drug metabolites.

Activity of maytansinoid metabolites. The two major metabolites, *S*-methyl-DM4 and lysine-N^{ϵ}-SMCC-DM1, were synthesized and tested for their *in vitro* cytotoxicity against COLO 205 cells and Namalwa cells. *S*-methyl-DM4 was highly cytotoxic with an IC_{50} value of 2 pmol/L against both cell lines, whereas lysine-N^{ϵ}-SMCC-DM1 was ~10^5-fold less potent against both cell lines with an IC_{50} value of 0.1 μmol/L (data not shown). This difference may be explained by the different charge status of the compounds. The charged lysine derivatives are expected to penetrate cell membranes very inefficiently such that high external concentrations are needed to reach the required toxic intracellular concentrations, whereas penetration of cell membranes is efficient for the neutral lipophilic *S*-methyl-DM4 compound.

Accumulation of the lysine-N^{ϵ}-SMCC-DM1 metabolite from the noncleavable conjugate is coincident with the observed formation of the potent *S*-methyl-DM4, DM4, and lysine-N^{ϵ}-SPDB-DM4 from the cleavable conjugate. This suggests that the lysine-N^{ϵ}-SMCC-DM1 metabolite is as potent as the metabolites from the cleavable conjugate when delivered intracellularly and that all of the maytansinoid metabolites are active when produced in the cell. The cell cycle arrest of both the cleavable and noncleavable conjugates was abrogated in the presence of the lysosomal inhibitor BafA1 (Fig. 1*C*). If the lysine-N^{ϵ}-SMCC-DM1 metabolite and the other metabolites observed from the cleavable conjugate arrest cells, BafA1 should prevent their formation. To investigate this possibility, COLO 205 cells were incubated at 37°C for 22 hours with 10^{-7} mol/L huC242-SMCC-[^{3}H]DM1 or huC242-SPDB-[^{3}H]DM4 conjugate in the presence or in the absence of 300 nmol/L BafA1. We found that BafA1 abolished the formation of both the lysine-N^{ϵ}-SMCC-DM1 from the thioether-linked conjugate, and the *S*-methyl-DM4 from the disulfide linked conjugate (Fig. 4*A*). In addition, no metabolites were detected in the medium of cells treated with either conjugate in the presence of BafA1 (data not shown). These results suggest that the lysine metabolites are toxic when delivered intracellularly and that lysosomal processing is necessary for the production of all the observed metabolites.

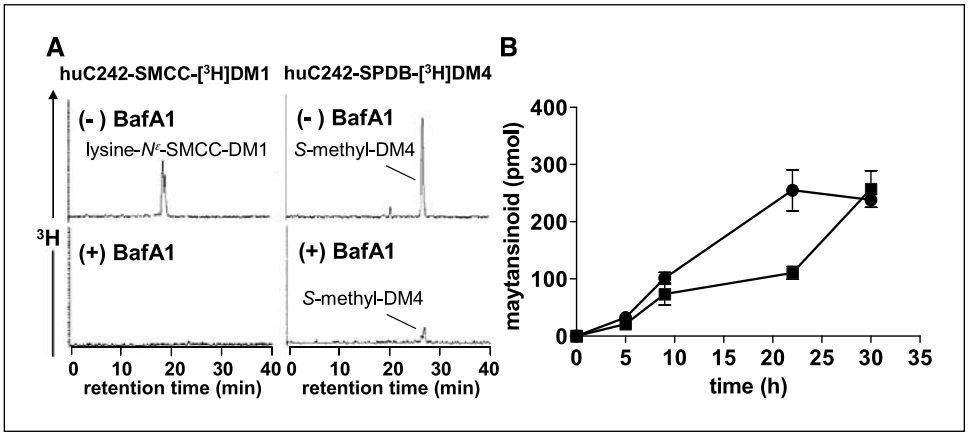

Figure 4. The role of the major metabolites in cellular toxicity. *A,* influence of BafA1 on the cellular metabolism of huC242-SMCC-[^{3}H]DM1 and huC242-SPDB-[^{3}H]DM4 in the presence or absence of BafA1. The chromatograms are from acetone extracts of COLO 205 cells treated with huC242-SMCC-[^{3}H]DM1 or huC242-SPDB-[^{3}H]DM4 for 22 hours in the presence of BafA1 or no treatment. *B,* accumulation of maytansinoid metabolites formed upon treatment of COLO 205 cells with huC242-SPDB-D-[^{3}H]DM4 versus huC242-SPDB-[^{3}H]DM4. Total amounts of maytansinoid metabolites generated from huC242-SPDB-D-[^{3}H]DM4 (*closed squares*) and from huC242-SPDB-[^{3}H]DM4 (*closed circles*). The metabolites were quantified as described in Fig. 2.

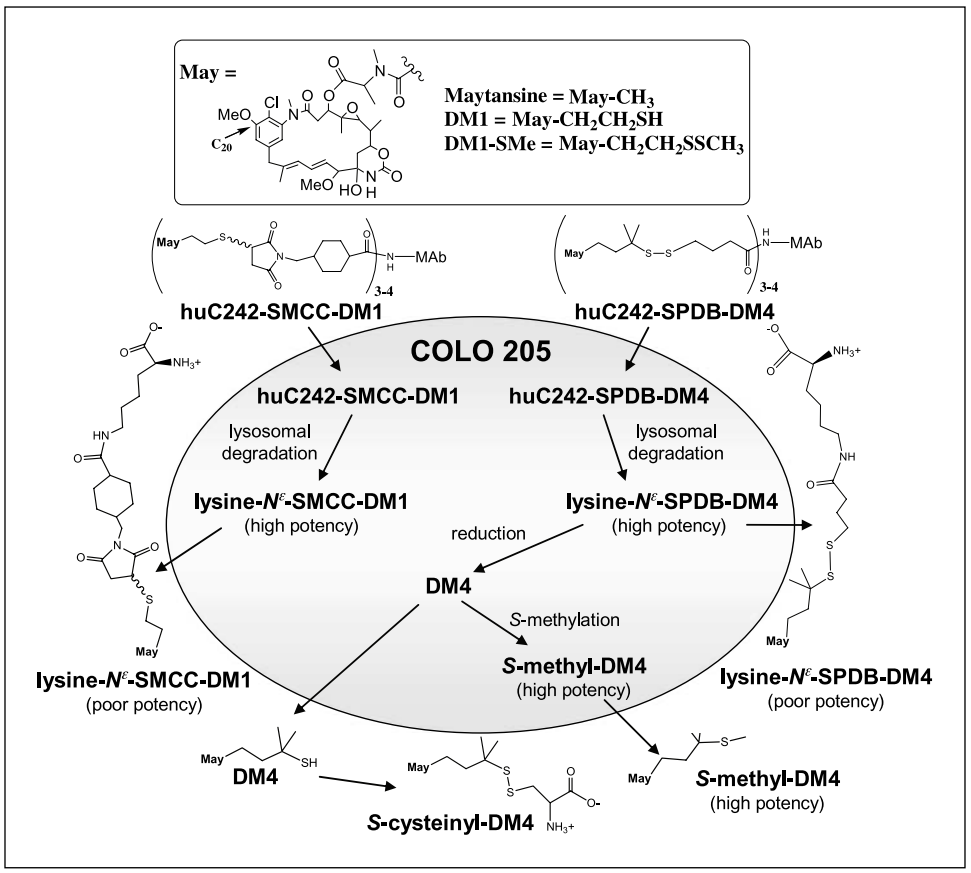

Figure 5. Model for the activation of huC242-maytansinoid in targeted cancer cells. The initial steps of conjugate activation are similar for the disulfide-linked conjugate huC242-SPDB-DM4 and the nondisulfide-linked conjugate huC242-SMCC-DM1. Both are first internalized by the target cancer cells via antigen-mediated endocytosis, delivered to lysosomes by the vesicular trafficking, and then degraded into the lysine derivatives, lysine-N^{ϵ}-SMCC-DM1 and lysine-N^{ϵ}-SPDB-DM4. These lysine derivatives likely bind to the intracellular target, tubulin, and cause cytotoxicity by the inhibition of microtubule polymerization. Unlike lysine-N^{ϵ}-SMCC-DM1, lysine-N^{ϵ}-SPDB-DM4 can undergo further intracellular modifications, reduction, and *S*-methylation, ultimately leading to the formation of *S*-methyl-DM4. Whereas the charged lysine derivatives are no longer active once they leave the target cells, the neutral lipophilic *S*-methyl-DM4 compound continues to be active and can reenter the target cells or enter neighboring cells (bystander).

The rate of release of total maytansinoids is approximately constant for 20 hours, yet few metabolites are observed in the medium until after 9 hours by which time the maximum amount of metabolites in the cell has been achieved (Fig. 3*A, c*). This suggests that the binding of metabolites to the intracellular target affects the rate of the efflux and that less toxic derivatives of DM4 may efflux at earlier times if the decreased toxicity is due to a lower binding affinity to the intracellular target. To investigate this possibility, the cellular processing of a conjugate was prepared from a 50-fold less potent (data not shown) isomer of DM4, D-[^{3}H]DM4. DM4 has the natural L-*N*-methyl-alanyl group in the side chain, whereas D-DM4 has its D-*N*-methyl-alanyl isomer. HuC242 conjugates prepared with the D-isomer of DM4 were at least 700-fold less toxic to COLO 205 cells than the corresponding L-isomer conjugate (data not shown). Samples of 2×10^6 COLO 205 cells were exposed to 10^{-7} mol/L huC242-SPDB-D-[^{3}H]DM4 conjugate and 10^{-7} mol/L huC242-SPDB-[^{3}H]DM4 as a control at 37°C for various periods of time and analyzed by reversed-phase HPLC (Supplementary Fig. S5). Almost no metabolites are observed in the cells treated with huC242-SPDB-D-[^{3}H]DM4 even after 30 hours, whereas an unknown metabolite with a retention time of 22 minutes was observed in the medium after only 5 hours of incubation and steadily increases after 9, 22, and 30 hours of exposure. We confirmed the identity of the unknown metabolite as lysine-N^{ϵ}-SPDB-D-DM4 by MS analysis (M + Na = 1,048.5).

The amount of the lysine-N^{ϵ}-SPDB-D-DM4 metabolite after 30 hours was similar to the sum of all the metabolites from the control cells treated with huC242-SPDB-[^{3}H]DM4 after 30 hours (Fig. 4*B*), suggesting that the two conjugates with the D and L isomers of DM4 are both internalized and processed to their respective lysine-DM4 adducts at similar rates. The explanation for the lack of an appreciable accumulation of D-DM4, *S*-cysteinyl-D-DM4, and *S*-methyl-D-DM4 from the conjugate with the *D* isomer of DM4 may be explained by poor intracellular binding and rapid efflux of lysine-N^{ϵ}-SPDB-D-DM4.

Discussion

Our results suggest a model for the activation of antibody-maytansinoid conjugates in target cells, depicted in Fig. 5. Both the disulfide-linked conjugate and the conjugate with the nondisulfide linker share a common initial process required for activation, involving receptor-mediated internalization of the conjugate-antigen complex into endosomes and subsequent fusion of the endosomal vesicle with the lysosomal compartment, ultimately leading to lysosomal degradation of the conjugates. The lysine-N^{ϵ}-SMCC-DM1, a product of proteolytic digestion of the antibody component of the conjugate, is the only metabolite present in measurable quantities in experiments with the thioether-linked conjugate. The analogous metabolite generated through this process from the disulfide-linked conjugate, lysine-N^{ϵ}-SPDB-DM4, was also identified, although in smaller quantities, because it likely plays a precursor role for the additional metabolites identified in the samples. Additionally, the total amount of all metabolites generated during the time of the experiments (22-30 hours) was the same for both conjugates and the accumulation occurred at similar rates. The importance of lysosomal degradation for conjugate activation is supported by the near-complete absence of metabolites upon

incubation of target cells with either of the two conjugates in the presence of the lysosomal inhibitor, BafA1 (Fig. 4*A*). We also found that the activation process includes an obligatory binding step of the conjugate to its target cell surface antigen, because only minor amounts of metabolites were generated from analogous antibody-maytansinoid conjugates that did not bind to COLO 205 cells.

Following the generation of lysine-N^{ϵ}-SMCC-DM1 and lysine-N^{ϵ}-SPDB-DM4 through lysosomal degradation, only the latter undergoes additional intracellular processing through reduction of the disulfide bond to produce DM4 and subsequent *S*-methylation to produce *S*-methyl-DM4. The sequential nature of these steps (Fig. 5) is supported by the kinetics of formation of these metabolites in cells treated with huC242-SPDB-DM4 (Fig. 3). In our experiments, we distinguish between metabolites inside the cells and those that had escaped into the culture medium. We observed that from both conjugates about equal quantities of maytansinoid metabolites were retained within the cells, reaching a maximum after ~9 hours of exposure of the cells to the conjugates, which was then maintained during the entire 26 hours of incubation. These results suggest that metabolites from both conjugates, principally lysine-N^{ϵ}-SMCC-DM1 from the thioether conjugate and *S*-methyl-DM4 from the disulfide-linked conjugate, bind to the same cellular target. This binding reaches a steady state after ~9 hours. This hypothesis is supported by the observation that no significant metabolites were retained inside cells treated with conjugate containing the nontoxic D-DM4 isomer. These results also indicate that the excess amount of the charged, hydrophilic metabolites, lysine-N^{ϵ}-SMCC-DM1 and lysine-N^{ϵ}-SPDB-DM4, and the other metabolites from the cleavable conjugate, are found entirely in the culture medium when produced at levels above this steady-state (saturated) level, suggesting that COLO 205 cells may efflux these maytansinoid derivatives via an active transport mechanism. Nevertheless, our results also suggest that saturation of the intracellular target of maytansinoid derivatives is achieved even in the context of this active efflux process. Studies to gain a better understanding of this phenomenon are ongoing in our laboratory.

The major maytansinoid species identified from the disulfide-linked conjugate, *S*-methyl-DM4, is the result of disulfide cleavage and subsequent methylation of the sulfhydryl group on DM4. The results discussed above suggest that the disulfide cleavage probably occurs after lysosomal digestion. The cleavage may even happen only after binding to the target protein because the primary metabolite formed from the conjugate with the D-isomer, lysine-N^{ϵ}-SPDB-D-DM4, was secreted into the medium and very little D-DM4 or *S*-methyl-D-DM4 was observed.

We isolated small amounts of the DM4 metabolite, which is the immediate product of cleavage of the disulfide bond. Most of the DM4 was rapidly methylated to the stable and potent *S*-methyl-DM4 derivative, which was the largest fraction in the metabolite mixture. It is likely that the methylation is catalyzed by a methyl transferase of which there is an abundance inside cells (20).

The major released, stable maytansinoid species from the disulfide-linked conjugate is the uncharged, lipophilic *S*-methyl-DM4 derivative, which was found to be highly toxic to cells. In contrast, the released maytansinoid from the thioether-linked conjugate is the charged lysine-N^{ϵ} -SMCC-DM1 derivative, which in the medium of cells had a very low cell killing potency, presumably due to its inability to cross the plasma membrane into the cell. These distinct properties of the two major forms of the released drugs might offer an answer to the conundrum of equal *in vitro* potency of both conjugates toward COLO 205 target cells and higher *in vivo* activity with the disulfide-linked conjugate in established s.c. COLO 205 tumor models. We have recently discovered (21) that disulfide-linked antibody maytansinoid conjugates can eradicate tumors in mice containing both antigen-positive and antigen-negative cells by bystander cytotoxicity. This process was not observed with thioether-linked maytansinoid conjugates, and we showed that it included the formation of a cytotoxic maytansinoid species that can penetrate cellular membranes. From the data presented here, we conclude that the charged lysine derivatives are no longer active once they leave the targets cells, whereas the neutral lipophilic *S*-methyl-DM4 compound continues to be active and can reenter the target cells or enter neighboring cells to induce bystander cytotoxicity. In established tumors *in vivo*, where antigen expression may be heterogeneous, or where access to the conjugate may not be equal for all cells due to a defective capillary system and other factors (for a review, see ref. 22), direct cytotoxicity of all cells by the conjugate may not be possible; thus, the *S*-methyl-DM4 metabolite may contribute greatly to the bystander potency and the anticancer effect of conjugates.

Acknowledgments

Received 12/20/2005; revised 2/1/2006; accepted 2/13/2006.

The costs of publication of this article were defrayed in part by the payment of page charges. This article must therefore be hereby marked *advertisement* in accordance with 18 U.S.C. Section 1734 solely to indicate this fact.

We thank John M. Lambert and Tom Chittenden for the many helpful suggestions and for their careful reading of the manuscript, and Rabih Gabriel, Charlene A. Audette, and Laura M. Bartle for the reagents and assistance.

References

1. Payne G. Progress in immunoconjugate cancer therapeutics. Cancer Cell 2003;3:207–12.
2. Wu AM, Senter PD. Arming antibodies: prospects and challenges for immunoconjugates. Nat Biotechnol 2005;23:1137–46.
3. Lambert JM. Drug-conjugated monoclonal antibodies for the treatment of cancer. Curr Opin Pharmacol 2005;5:543–9.
4. Bross PF, Beitz J, Chen G, et al. Approval summary: gemtuzumab ozogamicin in relapsed acute myeloid leukemia. Clin Cancer Res 2001;7:1490–6.
5. Cassady JM, Chan KK, Floss HG, Leistner E. Recent developments in the maytansinoid antitumor agents. Chem Pharm Bull (Tokyo) 2004;52:1–26.
6. Tolcher AW, Ochoa L, Hammond LA, et al. Cantuzumab mertansine, a maytansinoid immunoconjugate directed to the CanAg antigen: a phase I, pharmacokinetic, and biologic correlative study. J Clin Oncol 2003;21:211–22.
7. Chari RVJ, Martell BA, Gross JL, et al. Immunoconjugates containing novel maytansinoids: promising anticancer drugs. Cancer Res 1992;52:127–31.
8. Xie H, Audette C, Hoffee M, Lambert JM, Blättler WA. Pharmacokinetics and biodistribution of the antitumor immunoconjugate, cantuzumab mertansine (huC242–DM1), and its two components in mice. J Pharmacol Exp Ther 2004;308:1073–82.
9. Liu C, Tadayoni BM, Bourret LA, et al. Eradication of large colon tumor xenografts by targeted delivery of maytansinoids. Proc Natl Acad Sci U S A 1996;93:8618–23.
10. Firpo EJ, Koff A, Solomon MJ, Roberts JM. Inactivation of a Cdk2 inhibitor during interleukin 2-induced proliferation of human T lymphocytes. Mol Cell Biol 1994;14:4889–901.
11. Issell BF, Crooke ST. Maytansine. Cancer Treat Rev 1978;5:199–207.

12. Drose S, Altendorf K. Bafilomycins and concanamycins as inhibitors of V-ATPases and P-ATPases. J Exp Biol 1997;200:1–8.
13. Bowman EJ, Siebers A, Altendorf K. Bafilomycins: a class of inhibitors of membrane ATPases from microorganisms, animal cells, and plant cells. Proc Natl Acad Sci U S A 1988;85:7972–6.
14. van Weert AW, Dunn KW, Gueze HJ, Maxfield FR, Stoorvogel W. Transport from late endosomes to lysosomes, but not sorting of integral membrane proteins in endosomes, depends on the vacuolar proton pump. J Cell Biol 1995;130:821–34.
15. Oda K, Nishimura Y, Ikehara Y, Kato K. Bafilomycin A1 inhibits the targeting of lysosomal acid hydrolases in cultured hepatocytes. Biochem Biophys Res Commun 1991;178:369–77.
16. Zetser A, Levy-Adam F, Kaplan V, et al. Processing and activation of latent heparanase occurs in lysosomes. J Cell Sci 2004;117:2249–58.
17. Homewood CA, Warhurst DC, Peters W, Baggaley VC. Lysosomes, pH and the anti-malarial action of chloroquine. Nature 1972;235:50–2.
18. Singh R, Maloney EK. Labeling of antibodies by *in situ* modification of thiol groups generated from selenol-catalyzed reduction of native disulfide bonds. Anal Biochem 2002;304:147–56.
19. Ikegami S, Taguchi T, Ohashi M, Oguro M, Nagano H, Mano Y. Aphidicolin prevents mitotic cell division by interfering with the activity of DNA polymerase-α. Nature 1978;275:458–60.
20. Pacifici GM, Santerini S, Giuliani L, Rane A. Thiol methyltransferase in humans: development and tissue distribution. Dev Pharmacol Ther 1991;17:8–15.
21. Kovtun YV, Audette CA, Ye Y, et al. Antibody-drug conjugates designed to eradicate tumors with homogenous and heterogeneous expression of the target antigen. Cancer Res 2006;66:3214–21.
22. Carmeliet P, Jain RK. Angiogenesis in cancer and other diseases. Nature 2000;407:249–57.

Antibody-Maytansinoid Conjugates Are Activated in Targeted Cancer Cells by Lysosomal Degradation and Linker-Dependent Intracellular Processing

Hans K. Erickson, Peter U. Park, Wayne C. Widdison, et al.

Cancer Res 2006;66:4426-4433.